Hypersonic Speeds," *AIAA Journal*, Vol. 3, No. 6, June 1965, pp. 1001–1010.

[20] Softley, E. J. and Graber, B. C., "An Experimental Study of the Pressure and Heat Transfer on the Base of Cones in Hypersonic Flow," *AGARD Conference Proceedings*, No. 19, Vol. 1, May 1967.

[21] Bauer, A. B., "Some Experiments in the Near Wake of Cones," *AIAA Journal*, Vol. 5, No. 7, July 1967, pp. 1356–1358.

[22] Kavanau, L. L., "Base Pressure Studies in Rarefied Supersonic Flows," *Journal of the Aeronautical Sciences*, Vol. 23, No. 3, March 1956, pp. 193–208.

[23] Weiss, R. F., "Base Pressure of Slender Bodies in Laminar, Hypersonic Flow," *AIAA Journal*, Vol. 4, No. 9, Sept. 1966, pp. 1557–1559.

[24] Telionis, D. P., "Heat Transfer at Reattachment of a Compressible Flow over a Backward Facing Step with a Suction Slot," *AIAA Journal*, Vol. 10, No. 8, Aug. 1972, pp. 1108–1110.

DECEMBER 1973 AIAA JOURNAL VOL. 11, NO. 12

Numerical Analysis of Eddy Viscosity Models in Supersonic Turbulent Boundary Layers

J. S. SHANG,* W. L. HANKEY JR.,† AND D. L. DWOYER‡
Aerospace Research Laboratories, Wright-Patterson Air Force Base, Ohio

Three multilayer eddy viscosity models by Herring-Mellor, Cebeci-Smith-Mosinskis, and Maise-McDonald are compared in this investigation. The aforementioned models were incorporated into an implicit finite difference numerical scheme for compressible turbulent boundary layers. Calculations were performed over Mach number ranges of approximately 0 to 4.55 with the Reynolds number spanning the range of 4×10^6 to 1.41×10^9 for zero pressure gradient and adiabatic wall. All selected viscosity models produced comparable results and provided excellent agreement with the experimental measurements. The calculated results revealed the dominant nature of the viscous sublayer while modifications in the law of the wake region exhibited a relatively mild influence on the numerical solutions.

Nomenclature

C_f = skin-friction coefficient
C_p = specific heat at constant pressure
C = viscosity-density parameter
F = dimensionless velocity u/u_e
h = static enthalpy
k_1, k_2 = constants in eddy viscosity models
L = characteristic length
M = Mach number
P = pressure
Pr = Prandtl number $\mu C_p/\lambda$
T = static temperature
u, v = streamwise and normal velocity components
α = $u_e^2/C_p T_e$
β = $2\xi/u_e(du_e/d\xi)$
γ = ratio of specific heats
δ, δ^* = boundary-layer and displacement thickness
ε = kinematic eddy viscosity coefficient
$\bar{\varepsilon}$ = dimensionless equivalent viscosity $1+\varepsilon/\nu$
$\hat{\varepsilon}$ = dimensionless equivalent viscosity $1+(Pr/Pr_t)(\varepsilon/\nu)$
Θ = dimensionless temperature T/T_e
θ = boundary-layer momentum thickness
λ = molecular thermal conductivity
μ = molecular viscosity coefficient
ν = molecular kinematic viscosity
ξ, η = transformed streamwise and normal coordinates
ρ = density
τ = shear stress

Subscripts
e = denoted variable evaluated at local external stream
t = turbulent property
t,i = beginning of transition
t,f = end of transition
w = denoted variable evaluated at wall
$\langle\ \rangle$ = time-mean average

Presented as Paper 73-164 at the AIAA 11th Aerospace Sciences Meeting, Washington, D.C., January 10–12, 1973; submitted February 12, 1973; revision received July 5, 1973.

Index category: Boundary-Layer and Convective Heat Transfer—Turbulent.

* Aerospace Engineer, Hypersonic Research Laboratory. Member AIAA.

† Senior Scientist, Hypersonic Research Laboratory. Member AIAA.

‡ Captain, U.S. Air Force, Hypersonic Research Laboratory; presently Research Engineer, United Aircraft Research Laboratories, East Hartford, Conn. Student Member AIAA.

Introduction

THE primary purposes of this investigation was to evaluate the classic eddy viscosity model in the regions of the viscous sublayer, the law of the wall, and the law of the wake. Several multilayer eddy viscosity models were chosen for the present purpose. The choice of the classic flux-gradient concept over the turbulent kinetic energy method was based on the fact that for zero pressure gradient situations both methods yielded virtually identical results.[1] One recognizes that both methods could not escape the reign of phenomenological study of turbulent boundary layers. The common weakness manifested itself obviously in the prediction of flows which deviated from the "equilibrium" condition. For the aforementioned reason the present evaluation was restricted to the flows over an adiabatic flat plate.

The viscous sublayer models adopted in the present analysis included the works of Van Driest,[2] Mellor,[3] and McDonald.[4] Van Driest's work on the viscous layer yielded continuous velocity and shear distributions for turbulent flow near a smooth wall. Mellor studied the viscous layer in the light of the similarity law. Noting the different characteristic behavior in

various regions of the turbulent layer, he adopted an asymptotic matching scheme to develop a composite effective viscosity for the entire layer. The more recent work by McDonald on the viscous layer was prompted by the observations of Kline et al.[5] in the wall region. An intermittent representation of the turbulent flow in the sublayer was approximated by the normal probability function. All the cited viscous sublayer models represented a modification of the law of the wall immediately adjacent to the wall. The logarithmic portion of the turbulent boundary layer, as described by the Prandtl mixing-length concept, was employed for all cases in the present analysis.

In the law of the wake region the Clauser defect law, the Cebeci-Smith-Mosinskis[6] intermittency correction and the Maise-McDonald[7] correction were selected for the present purpose. The Maise-McDonald eddy viscosity model was deduced from their generalized velocity profile which contained the law of the wall and the law of the wake by an integral momentum scheme.

The concept of eddy viscosity has been successfully applied to compressible turbulent boundary layers by means of finite difference schemes; however, uncertainties remained in the numerical accuracy and on the influence of the transition region. In the present analysis, the former was resolved by a systematic study of the numerical errors related to grid-point size. The effect of the initial condition on the transition region was investigated by the Dhawan and Narasimha's[8] transition model. The transition model was first evaluated by comparison with experimental data. The effect of initial condition was then obtained by comparing two numerical solutions.

Governing Equations

The compressible, turbulent boundary-layer equations for two-dimensional flows were expressed as[9,10]

$$(\partial/\partial x)(\rho u)+(\partial/\partial y)(\rho v+\langle\rho' v'\rangle)=0 \tag{1}$$

$$\rho u\frac{\partial u}{\partial y}+(\rho v+\langle\rho' v'\rangle)\frac{\partial u}{\partial y}=\rho_e u_e\frac{du_e}{dx}+\frac{\partial}{\partial y}\left(\mu\frac{\partial u}{\partial y}-\rho\langle u'v'\rangle\right) \tag{2}$$

$$\rho u\frac{\partial h}{\partial x}+(\rho v+\langle\rho' v'\rangle)\frac{\partial h}{\partial y}=-u\rho_e u_e\frac{du_e}{dx}+\frac{\partial}{\partial y}\left(\frac{\lambda}{C_p}\frac{\partial h}{\partial y}\right)+\mu\left(\frac{\partial u}{\partial y}\right)^2+\frac{\partial}{\partial y}(-C_p\rho\langle v'T'\rangle)-(\rho\langle u'v'\rangle)\frac{\partial u}{\partial y} \tag{3}$$

The x, y coordinates formed a curvilinear system as in the classic boundary-layer analysis. The x coordinate denoted the distance on the contour measured from the leading edge and y was the coordinate orthogonal to the contour.

The validity of the approximate equations of motion for compressible turbulent boundary layer had been scrutinized by Van Driest,[9] and more recently by Herring et al.[10] Morkovin,[11] and Bradshaw.[12] The additional assumption beside the classical boundary-layer approximation was that of the relative smallness of the terms involving the density fluctuation. The order-of-magnitude arguments made either by assuming $\rho' u_e^2 \ll \rho_e u_e^2$ (Bradshaw[12]) or $\rho_e u_e^2 \ll p_e$ (Morkovin[11]) led to the requirements of $0[(\gamma-1)M_e^2]\sim 0(1)$ or $M_e \leqq 5$ (Ref. 11). For compressible turbulent boundary layers in mild pressure gradients, Bradshaw showed a more restrictive condition $(\gamma-1)M_e^2\, d\delta/dx \ll 1$.

Three time-mean fluctuation terms appearing in the system of equations were usually designated as apparent mass flux $\langle\rho' v'\rangle$, momentum flux $\rho\langle u'v'\rangle$, and energy flux $C_p\rho\langle v'T'\rangle$ due to turbulence. Analytically, the additional dependent variables prevented the closure of the system of equations to describe turbulent boundary-layer flows. The balance of the variables and equations could only be achieved through various assumptions.

In order to achieve the closure of this system of equations, an assumption concerning the apparent transport properties was made. The apparent mass flux term $\langle\rho' v'\rangle$ was relatively easy to take into account under the boundary-layer assumption. We defined the velocity component normal to the surface as

$$\tilde{v}\equiv v+\langle\rho' v'\rangle/\rho \tag{4}$$

The eddy viscosity concept yielded

$$-\rho\langle u'v'\rangle=\rho\varepsilon\,\partial u/\partial y \tag{5}$$

If one accepted the hypothesis of eddy viscosity for the Reynolds stress, it would be logical to extend this concept to the apparent heat flux term. As previously defined

$$-\rho\langle v'T'\rangle\equiv(1/C_p)\lambda_t\,\partial T/\partial y \tag{6}$$

It follows naturally at this stage to define the turbulent Prandtl number as

$$Pr_t=\frac{C_p\varepsilon}{\lambda_t}\equiv\frac{\langle u'v'\rangle}{\langle v'T'\rangle}\frac{(\partial T/\partial y)}{(\partial u/\partial y)} \tag{7}$$

Finally, we obtained the closure of the governing equations by introducing the perfect gas law and Sutherland's viscosity equation. The associated boundary conditions were the nonslip conditions; adiabatic wall and asymptotic behavior of velocity and temperature to the freestream condition. The Levy-Lees transformation converted the governing equations into

$$\bar{v}_\eta+2\xi F_\xi+F=0 \tag{8}$$

$$(C\bar{\varepsilon}F_\eta)_\eta-\bar{v}F_\eta+\beta(\Theta-F^2)=2\xi FF_\xi \tag{9}$$

$$[(1/Pr)C\bar{\varepsilon}\Theta_\eta]_\eta-\bar{v}\Theta_\eta+\alpha C\bar{\varepsilon}F_\eta^2=2\xi F\Theta_\xi \tag{10}$$

where $\bar{v}$ was defined as

$$\bar{v}=(2\xi/\rho_e u_e\mu_e)[(\partial\eta/\partial x)F+\rho\tilde{v}/(2\xi)^{1/2}]$$

The system of equations was similar to that of Harris'[13] with the exception that transverse curvature terms were not considered here.

The Eddy Viscosity Models

The turbulent boundary layer was known to possess widely different length scales. The distinctive regions of the eddy viscosity models usually are described as consisting of three layers, namely the viscous layer, the law of the wall and the law of the wake region. The various regions might have different designations but all modifications merely intend to take into account the intermittent nature of turbulence in the boundary layer. The existence of the viscous sublayer immediately adjacent to the wall has long been recognized. The structure of the viscous layer was investigated by Laufer[14] and more recently by Kline et al.[5] The thin wall region plays a very dominant role in determining the structure of the entire boundary layer. The outer portion of a turbulent layer on the other hand, has a wakelike structure in that there is great similarity due to the effects of intermittency, entrainment and the sensitivity of the outer portion of the profile to pressure gradient.[15] In the framework of an eddy viscosity concept, one could describe the equivalent viscosity by different inner and outer values. The outer region then included only the law of the wake region. The equivalent eddy viscosity could be given as $\nu+\Gamma\varepsilon_i$ and $\nu+\Gamma\varepsilon_0$ in the inner and outer regions, respectively. The function Γ was the transition factor which assumed a value of zero in the laminar flow and became unity downstream of the transition zone.

In the sublayer region we selected three models:

Cebeci-Smith-Mosinskis model

$$\left(\frac{\varepsilon}{\nu}\right)_i=k_1^2\frac{y^2}{\nu}\left\{1-\exp\left[-\frac{\nu}{26\nu}\left(\frac{\tau w}{\rho}+\frac{dp}{dx}\frac{y}{\rho}\right)^{1/2}\right]\right\}^2\left|\frac{\partial u}{\partial y}\right| \tag{12}$$

Herring and Mellor model

$$(\varepsilon/\nu)_i=\chi^4/[\chi^3+(6.9)^3] \tag{13}$$

where

$$\chi=(k_1 y/\nu)(\tau/\rho)^{1/2}$$

McDonald model

$$(\varepsilon/\nu)_i=k_1^2(y^2/\nu)P(\zeta)\left|\partial u/\partial y\right| \tag{14}$$

where $P(\zeta)$ was the normal probability function

$$\zeta=\frac{(y/\nu)(\tau/\rho)^{1/2}-23}{8}$$

One observes that the scaling variable in Mellor's and McDonald's models is the local τ instead of τ_w as in Cebeci-Smith-Mosinskis' model. The numerical differences between the Mellor and Cebeci models were minor because both models were evaluated from Laufer's[14] data. However, conceptually the two models were vastly different. Cebeci's model was a derivative of Van Driest's analysis of the wall regions, the exponential damping was the asymptote of a time dependent Stokes solution. Mellor's model, however, was obtained by similarity consideration. The McDonald model was simply a modification for the intermittent turbulence in the viscous sublayer.[4] In the law of the wall region, the eddy viscosity model was simply described by the Prandtl mixing length concept. In Mellor's terminology it was denoted as the overlapping region

$$\varepsilon/\nu = (k_1{}^2 y^2/\nu)|\partial u/\partial y| \tag{15}$$

For the law of the wake or the defect law region we selected the modified Clauser defect law and Maise-McDonald's modification.

$$(\varepsilon/\nu)_0 = k_2 u_e(\delta_i{}^*/\nu)\cdot\gamma(y/\delta) \tag{16}$$

The basic scaling of $\delta_i{}^*$ for compressible flow was adopted by Herring et al. and Cebeci et al. Cebeci et al., in addition, included the intermittency correction factor γ obtained by Klebanoff.[16] Cebeci et al. used the approximate expression for the error function to give

$$\gamma = [1+5.5(y/\delta)^6]^{-1} \tag{17}$$

The Maise-McDonald[7] eddy viscosity model was deduced from the integral momentum method by their generalized velocity profile for a compressible turbulent layer over an adiabatic flat plate. They demonstrated that the calculated kinematic eddy viscosity was nearly independent of Mach number, if normalized with respect to the incompressible displacement thickness and the freestream velocity. The effects of Reynolds number on the kinematic viscosity was less pronounced than the Mach number. In the spirit of seeking a simple kinematic eddy viscosity model, the effect of Reynolds number was not taken into consideration for the present investigation. Maise-McDonald's model was introduced into the numerical procedure in tabulated form. The rest of the calculation procedures and associated initial conditions remained unchanged between these models. In order to take into account the Mach number effects on Maise-McDonald's kinematic eddy viscosity model, a three-point interpolation scheme was utilized to obtain the eddy viscosity coefficient from their published data.[7]

The initial conditions for a turbulent boundary-layer investigation often provoked uncertainty. The issue always evolved from the laminar-turbulent transition phenomena. The Reynolds number of turbulent flows usually was calculated by the approximate location of the virtual origin.[16,17] In numerical analyses the initial conditions either allowed the eddy viscosity to become nonzero[6] at some specified location or to be by-passed completely with empirical information.[10,12] The present analysis attempted to investigate the initial conditions by using the transition model of Dhawan and Narasimha.[8] The transition model was successfully introduced to compressible flow by Harris.[13]

The transition model was

$$\Gamma(\bar{x}) = 1-\exp(-0.412\bar{x}^2) \tag{(18)}$$

where $\bar{x}$ is the normalized streamwise coordinate in the transition region.

$$\bar{x} = [(x-x_{t,i})/\Lambda] \qquad x_{t,i} \leqq x \leqq x_{t,f} \tag{19}$$

$x_{t,i}$ and $x_{t,f}$ denoted the initial and final locations of the transition zone. Λ is a measure of the extent of the transition region defined by

$$\Lambda = x_{\Gamma=3/4} - x_{\Gamma=1/4} \tag{20}$$

In the aforementioned model, three parameters are required, namely $x_{t,i}$, $x_{t,f}$ and $x_{\Gamma=1/4}$ (or $x_{\Gamma=1/4}$). For the present purpose, the extent of transition was obtained from experimental data. The parameter Λ was allowed to vary until agreement with experimental data was reached. This systematic variation yielded a parametric study of initial conditions for the present calculations. Matting's[17] data was selected for the study, and application of the transition model was also limited to Matting's data.

Current investigations of the energy transport process have not reached a comparable state of development as that of the Reynolds stress. For simplicity the present analysis utilized a constant turbulent Prandtl number of 0.9. However, provisions were also made in the numerical scheme to include more sophisticated models for future development.

Numerical Solution of the Governing Equations

The linearization and solution technique in the present analysis followed closely the works of Flugge-Lotz, Blottner, and Davis.[18,19] A three-point difference scheme treated derivatives in the ξ direction by a Taylor series expansion around the unknown ray $m+1$ to upstream rays m, and $m-1$. The derivatives with respect to η were expanded, respectively, about a central point n. The momentum and energy equations in finite difference form were solved simultaneously.

To facilitate the calculations, variable step size was incorporated into the numerical procedure. In the ξ direction, double step sizes were selected at various streamwise stations to speed up calculation. In the η direction, additional stretching of the η coordinate was implemented. The geometric progression in successive $\Delta\eta_n$ was identical to that of Cebeci et al.[6]

$$\Delta\eta_n = k^{n-1}\Delta\eta_1 \qquad n = 1,2,\ldots,N \tag{21}$$

In the present analysis, the maximum streamwise step size was around $x/L = 0.01$. The step size in the η direction was more restrictive. It was found that the most suitable initial step size was about $\Delta\eta_1 = 0.0005$. Further decrement in $\Delta\eta_1$ by a factor of two merely affected the skin friction coefficient by $\frac{1}{10}\%$.

The initial conditions used in this numerical scheme were similar to that of Cebeci et al. and Harris. Laminar similar solutions were generated in the program at the first two stations. At these stations, the $\Delta\xi/L$ should be approximately $\Delta\xi/L = 0.0006$ to minimize the possible errors downstream.

An iteration procedure for the nondimensional velocity and temperature profiles was included in the present scheme. The initial profiles in the iteration process were predicted by a straightforward difference scheme. The profiles were then allowed to relax until no change between iterations occurred. Aside from the fact that this process assures the convergence of the

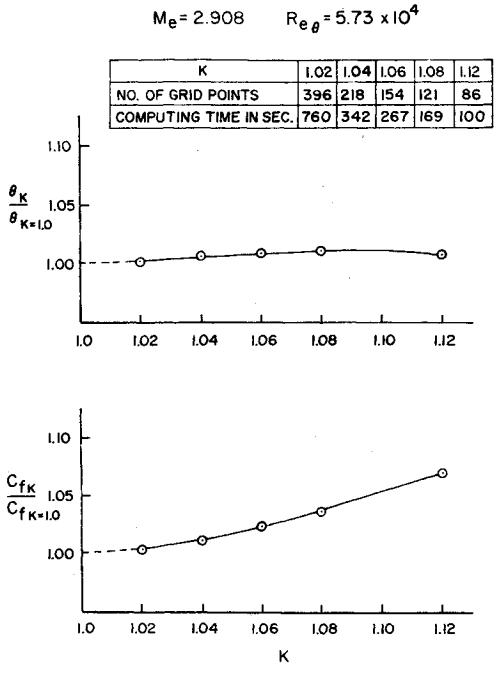

Fig. 1 Numerical errors vs grid-point spacing.

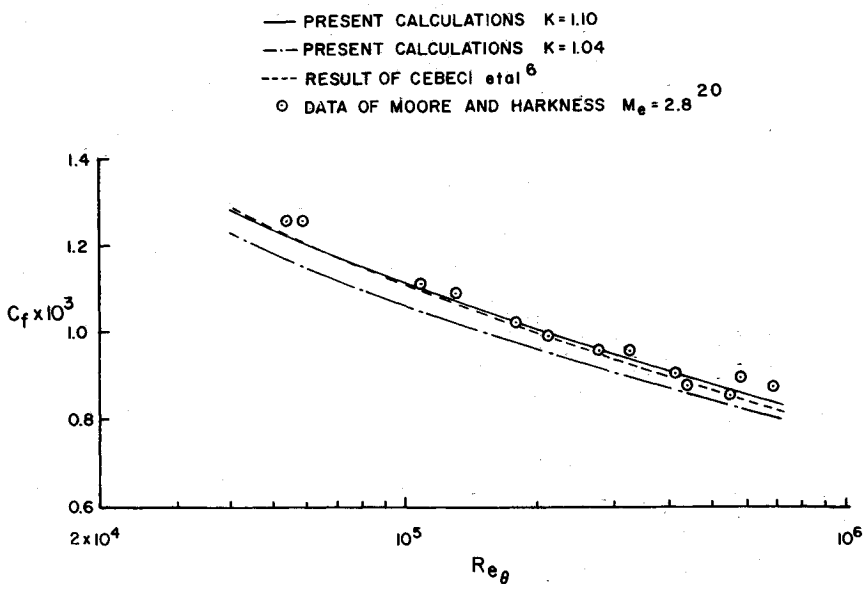

Fig. 2 The effect of geometrical progression constant k on the numerical accuracy.

solution, we consider this process significant since the eddy viscosity models scale themselves according to the mean flow properties, (gradients) particularly in the region adjacent to the wall. The tolerances adopted in this analysis for F and Θ were given a constant value of 0.00005 for all the calculations. The iteration procedure was not included in Harris' work.[13]

The shear stress and heat transfer at the wall were evaluated from transformed velocity and temperature profiles by a four-point difference scheme. Harris'[13] three point mean of the eddy viscosity function was used in the present analysis to prevent possible wavy distribution in eddy viscosity across the boundary layer. One would expect it to occur only in the discrete joint of Cebeci's outer and inner viscosity models.[6] However, the averaging process was retained in the program for calculations with Maise-McDonald's eddy viscosity model to isolate the comparison only to the eddy viscosity models.

The calculations were carried out by the CDC 6600 digital computer. Each iteration cycle required 0.4 sec to compute 250 grid points in the η coordinate. The computing time was roughly in linear proportion to the number of grid points in η. For example, 150 grid points in η coordinate required only 0.22 sec to complete the calculation cycle. The maximum number of profile iterations was about ten and was always associated with the starting condition and transition region.

Discussion of Results

The presentation of the computed results is organized into three groups. The first portion of the results is concerned with the relationship between numerical accuracy and the number of grid points (grid-point size). The second subject was focused on the effects of the transition criteria or initial conditions on the numerical solution. The rest of the efforts were devoted to the comparison of the various eddy viscosity models and the sensitivity of the models on the global boundary-layer properties.

Numerical errors of the finite difference analysis probably were reflected by the approximation of the truncated series expansion which in turn were governed by the step size. The constant k of the geometric progression for $\Delta\eta$ [Eq. (21)] played a significant role on computing time and numerical accuracy. The value of k was an index of the number of grid points in η. For example, at $Re_x = 1.41 \times 10^9$, $M_e = 2.8$ and $\Delta\eta_i/L = 0.0005$, $k = 1.12$ and $k = 1.04$ produced a number of grid points of 112 and 294, respectively. Figure 1 presents the calculated skin-friction coefficients and momentum thickness for various k values. One observes a maximum error in C_f of about 7% for $k = 1.12$ which corresponded to the minimum number of grid points for the tested case. The deviation in momentum thickness, however, was found to be insignificant. The calculated skin-friction coefficients are presented in Fig. 2 together with Cebeci's result and Moore-Harkness' data.[20] The agreement was excellent between experimental measurements, Cebeci's result, and the present calculation with 112 grid points. The more accurate calculation of C_f performed by assigning 294 grid points in η, however, revealed uniform underprediction of about 5%.

The laminar-turbulent transition model of Dhawan et al. was adopted to investigate the initial conditions for the turbulent boundary-layer calculations. Figure 3 shows the comparison between the experimental data of Matting et al., and the present prediction method at Mach numbers of 2.95 and 4.2. The transition model was satisfactory in describing the transition behavior. The eddy viscosity model of Cebeci et al. was adopted for the analysis of transition. The maximum discrepancy between the data and the calculation was located downstream of transition, and the calculated C_f was persistently overpredicted by around 6%.

The effects of the initial condition was studied by comparison of two similar calculations. One of the calculations was made

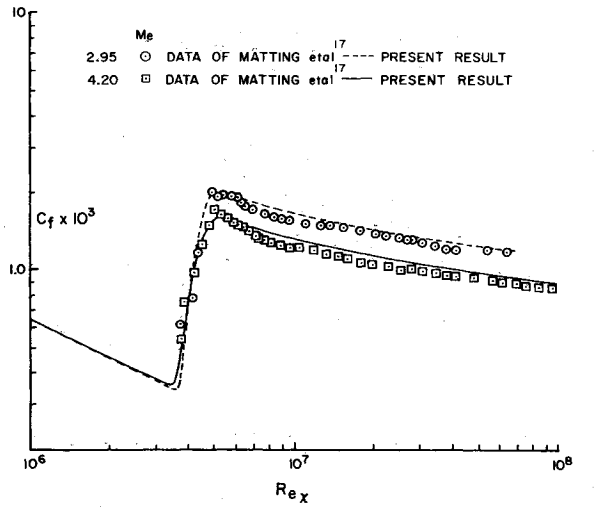

Fig. 3 Skin-friction distribution for laminar, transition, and turbulent flow regions.

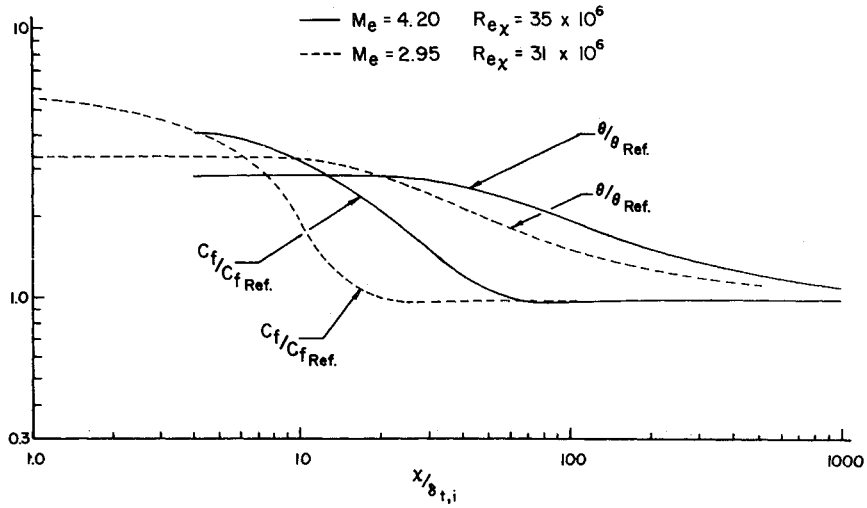

Fig. 4 Effect of the initial conditions on numerical calculations.

to become turbulent at the first station, the other one was calculated with the laminar-turbulent transition model closely following the experimental data. The ratio of C_f and momentum thickness θ for these two situations vs the normalized streamwise distance is given in Fig. 4. One observes that the C_f value is relatively insensitive to the initial condition, in that the difference between the two calculations vanishes around one hundred $\delta_{t,i}$ downstream of the beginning of transition. On the other hand, the momentum thickness was rather sluggish in attaining agreement between the two calculations.

In Fig. 5 three of the law of the wake eddy viscosity models are presented. To achieve the comparison, the sublayer region and the law of the wall region were calculated by the Van Driest modification of the wall region and Prandtl's eddy viscosity model, respectively. The Maise-McDonald law of the wake correction and Cebeci et al. intermittency correction in principle were identical, both intended to describe the intermittently turbulent behavior of the outer portion of the turbulent boundary layer. Regardless of the difference in the law of the wake region, the equivalent viscosity remained identical for the rest of the boundary layer. In contrast, the Clauser defect law representation excluding the intermittency correction increased the equivalent viscosity in the wall region and attenuated the extent of the logarithmic region. The accompanying velocity profiles are given in Fig. 6. Comparison of the numerical results with Klebanoff's data reveals the significance of the intermittency correction in the law of the wake region. The difference between results of Cebeci et al. and Maise et al. was found to be negligible.

The sublayer models were also similarly investigated. The Maise-McDonald eddy viscosity distribution was modified by Van Driest's, Mellor's and McDonald's viscous sublayer models. It was obvious that the sublayer model dominated the development of the turbulent boundary-layer structure. The sublayer not only determines the shear stress at the wall but scales the entire turbulent boundary layer (Fig. 7). The original Maise-McDonald eddy viscosity model without the consideration of the sublayer yielded similar results to the combination of Prandtl's and Clauser's eddy viscosity models. The McDonald viscosity model near the wall differs from the Mellor and Van Driest modification. The damping factor of McDonald's modification near the wall was nonzero by the description of the normal probability function but the modification produced similar results to that of Mellor and Van Driest.

We found that over the Mach number range of 0 to 4.55 and

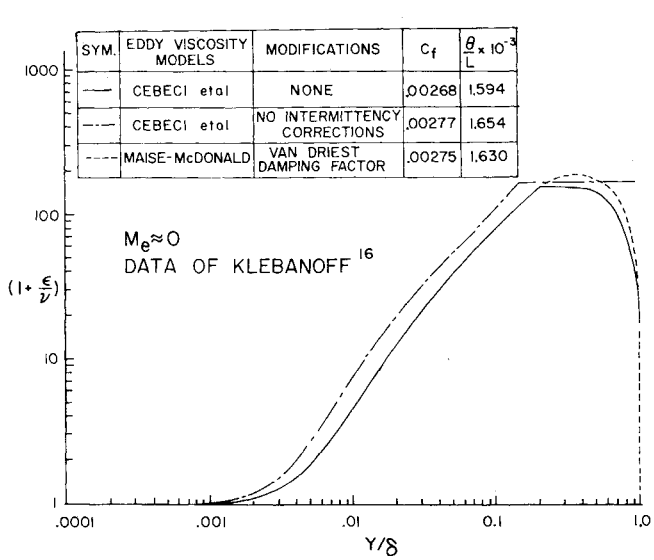

Fig. 5 Comparison of the intermittency correction in the law of the wake region.

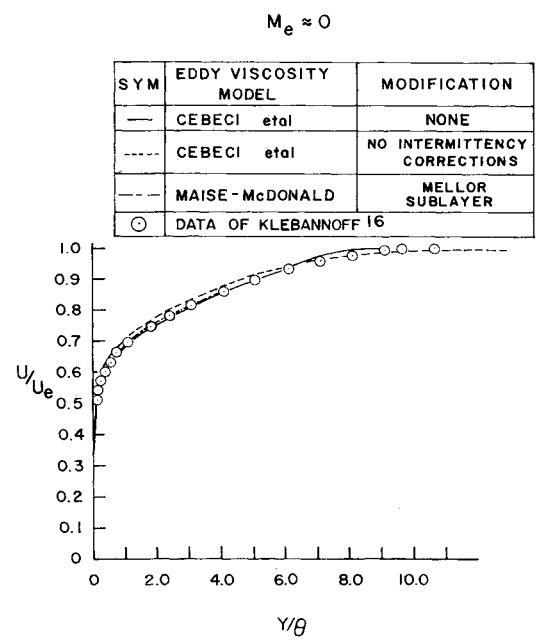

Fig. 6 Comparison of the calculated velocity profiles with Klebanoff's data.

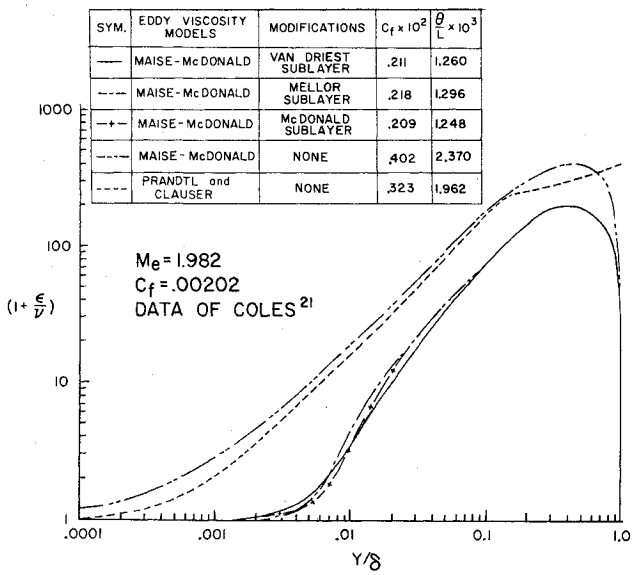

Fig. 7 Comparison of the viscous sublayer eddy viscosity models.

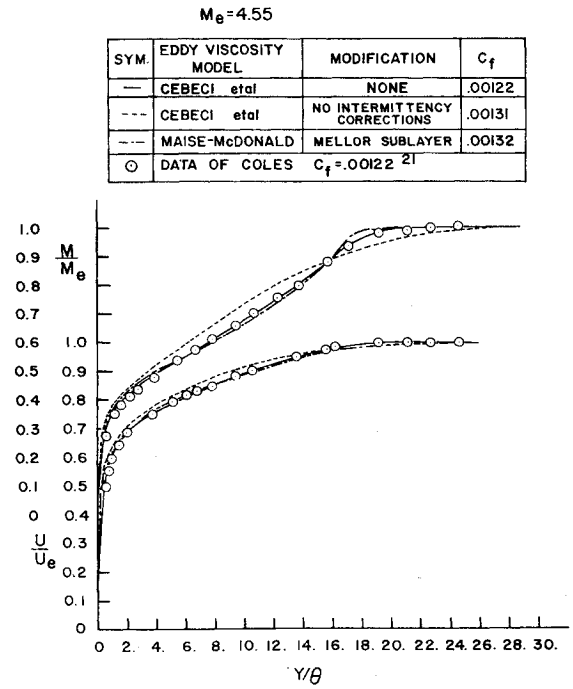

Fig. 9 Comparison of the calculated velocity and Mach number profiles with Coles' data ($M_e = 4.554$).

Reynolds number from 4×10^6 up to 1.41×10^9, the viscous sublayer was confined to within 0.015 of the local boundary-layer thickness. However, the influence of sublayer viscosity model was overwhelming in the finite difference calculations. In Figs. 8 and 9, we presented the calculated velocity and Mach number profile with various combinations of the sublayer and the law of the wake models. The comparisons were made with Coles' data[21] at Mach numbers of 1.982 and 4.55. Again one observed that the results of modified Maise-McDonald's viscosity model were virtually identical to that of the model of Cebeci et al. Observable deviations from the experimental data were obtained from the eddy viscosity model without intermittency correction. However,

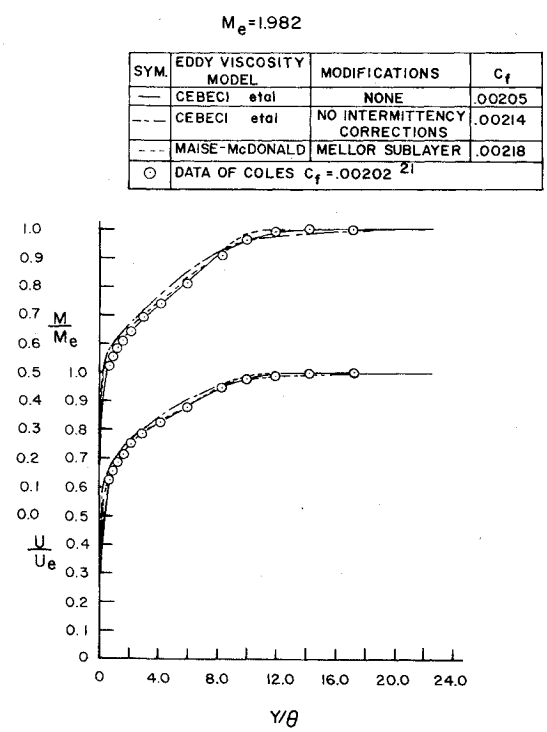

Fig. 8 Comparison of the calculated velocity and mach number profiles with Coles' data ($M_e = 1.982$).

the effect of the intermittency correction was not limited to the outer portions of the boundary layer. This might be attributable to the flow history aspect of the solving scheme.

All the demonstrated cases in the present analysis were restricted to the zero pressure gradient, adiabatic or near adiabatic flow conditions and the freestream Mach numbers were less than five. Therefore, the flowfields considered were near equilibrium or in a self-preserving condition and the terms associated with the density fluctuation were relatively small. The present calculations probably presented the best result that an eddy viscosity model could produce. Application of the eddy viscosity model to flowfields substantially different from the aforementioned, particularly, in cases of severe pressure gradient, significant amounts of heat transfer and hypersonic Mach numbers, may result in serious error. In essence, the eddy viscosity model shall only be used where the scaling lengths, either in the inner or the outer region of the eddy viscosity model, were originally devised.

Conclusions

The classic eddy viscosity models were investigated by comparison of three viscous sublayer models and two intermittency corrections in the outer portion of the turbulent boundary layer. For the cases examined, the three different viscous layer models produced a variation of less than 9% in C_f. However, neglect of the sublayer resulted in an overprediction of the skin-friction coefficient by about 90%. The thin viscous sublayer region not only directly affected the shear stress calculation, but also scaled the entire turbulent boundary layer. The von Kármán constant k_1 was parametrically changed and a 1% increase in k_1 resulted in +0.9% increase in C_f. The identical variation of k_2, Clauser constant, yielded only +0.4% change of C_f. The influence of k_1 and k_2 on the momentum thickness was less pronounced. The calculated results revealed an insensitivity to any intermittency correction in the law of the wake region. The difference between Maise-McDonald's and Cebeci-Smith intermittency correction was about 25% at a y/δ around 0.4 and yet the predicted skin-friction coefficients differed by only about 3%. However, the influence of the intermittency correction was not

confined to the outer portion of the turbulent boundary layer. For a turbulent boundary layer over an adiabatic flat plate, the sublayer was confined to within 0.015 of the boundary layer thickness. The logarithmic region was limited to 0.015 to 0.2 of the boundary layer, while the law of the wake region extended over the rest of the boundary layer. In addition, the distribution of three distinct regions of the turbulent boundary layer was essentially independent of the freestream Mach number for the calculated cases.

The transition model of Dhawan et al. was found adequate to describe the laminar-turbulent transition phenomena for compressible flows. Based upon the transition model, it was found that both the skin-friction coefficient and velocity profile were relatively insensitive to the transition location but the momentum thickness was profoundly affected. Obviously, the accuracy of predicted momentum thickness is dependent upon the relative location of transition. But if one accepts a fixed tolerance, the momentum thickness requires an order-of-magnitude larger downstream distance to attain the tolerance than that of the skin-friction coefficient.

References

[1] Mellor, G. L. and Herring, H. J., "Two Methods of Calculating Turbulent Boundary Layer Behavior Based on Numerical Solutions of the Equations of Motion," *Proceedings of 1968 AFOSR-IFR-Stanford Conference on Computation of Turbulent Boundary Layers,* Vol. I, Stanford Univ., Stanford, Calif., pp. 331–345.

[2] Van Driest, F. R., "On Turbulent Flow Near a Wall," *Journal of the Aeronautical Sciences,* Vol. 23, No. 11, 1956, pp. 1007–1011.

[3] Mellor, G. L., "The Effects of Pressure Gradients on Turbulent Flows Near a Smooth Wall," *Journal of Fluid Mechanics,* Vol. 24, Pt. 2, 1966, pp. 255–274.

[4] McDonald, H. M. and Fish, R. W., "Practical Calculations of Transitional Boundary Layers," Rept. L110887-2, March 1972, United Aircraft Research Lab., East Hartford, Conn.

[5] Kline, S. J., Reynolds, W. C., Schraub, F. A., and Runstalder, P. W., "The Structure of Turbulent Boundary Layers," *Journal of Fluid Mechanics,* Vol. 30, Pt. 4, 1967, pp. 741–773.

[6] Cebeci, T., Smith, A. M. O., and Mosinskis, G., "Calculation of Compressible Adiabatic Turbulent Boundary Layers," *AIAA Journal,* Vol. 8, No. 11, Nov. 1970, pp. 1974–1982.

[7] Maise, G. and McDonald, H., "Mixing Length and Kinematic Eddy Viscosity in a Compressible Boundary Layer," *AIAA Journal,* Vol. 6, No. 1, Jan. 1968, pp. 73–80.

[8] Dhawan, S. and Narasimha, R., "Some Properties of Boundary-Layer Flow During the Transition From Laminar to Turbulent Motion," *Journal of Fluid Mechanics,* Vol. 3, Pt. 4, 1958, pp. 418–436.

[9] Van Driest, E. R., "Turbulent Boundary Layer in Compressible Fluids," *Journal of the Aeronautical Sciences,* Vol. 18, No. 3, 1951, pp. 145–160, 216.

[10] Herring, H. J. and Mellor, G. L., "A Method of Calculating Compressible Turbulent Boundary Layers," CR-1144, Sept. 1968, NASA.

[11] Morkovin, M. V., "Effects of Compressibility on Turbulent Flow," *International Symposium on the "Mécanique de la Turbulence," Centre National de la Recherche Scientifique,* Paris, France, 1962, pp. 367–380.

[12] Bradshaw, P. and Ferris, D. H., "Calculation of Boundary-Layer Development Using the Turbulent Energy Equation: Compressible Flow on Adiabatic Walls," *Journal of Fluid Mechanics,* Vol. 46, Pt. I, 1971, pp. 83–110.

[13] Harris, J. E., "Numerical Solution of the Equations for Compressible Laminar, Transitional, and Turbulent Boundary Layers and Comparison with Experimental Data," TR T-368, 1971, NASA.

[14] Laufer, J., "The Structure of Fully Developed Pipe Flow," Rept. 1174, 1954, NACA.

[15] Coles, D., "The Law of the Wake in the Turbulent Boundary Layer," *Journal of Fluid Mechanics,* Vol. 1, Pt. 2, 1956, pp. 191–226.

[16] Klebanoff, P., "Characteristics of Turbulence in a Boundary Layer with Zero Pressure Gradient," TN 3178, 1954, NACA.

[17] Matting, F. W., Chapman, D. R., and Nyholm, J. R., "Turbulent Skin Friction at High Mach Numbers and Reynolds Numbers in Air and Helium," TR R-82, 1961, NASA.

[18] Flugge-Lotz, I. and Blottner, F. G., "Computation of the Compressible Laminar Boundary Layer Flow Including Displacement Thickness Interaction Using Finite-Difference Methods," AFOSR-2206, 1962, Air Force Office of Scientific Research, Washington, D.C.

[19] Davis, R. T. and Flugge-Lotz, I., "Laminar Compressible Flow Past Axisymmetric Blunt Bodies," TR143, 1963, Div. of Engineering Mechanics, Standord Univ., Stanford, Calif.

[20] Moore, D. R. and Harkness, J., "Experimental Investigations of the Compressible Turbulent Boundary Layer at Very High Reynolds Numbers," *AIAA Journal,* Vol. 3, No. 4, April 1965, pp. 631–638.

[21] Coles, D., "Measurements in the Boundary Layer on a Smooth Flat Plate in Supersonic Flow, Part III—Measurements in a Flat Plate Boundary Layer at the Jet Propulsion Laboratory," Rept. ND 20-71, 1953, California Inst. of Technology, Pasadena, Calif.